Chemical states of dodecanethiolate-passivated Au nanoparticles: synchrotron-radiation photoelectron spectroscopy

Tanaka, Akinori
Takeda, Yuitsu
Nagasawa, Tazumi
Takahashi, Kazutoshi

(Citation)
Solid State Communications,126(4):191-196

(Issue Date)
2003-04

(Resource Type)
journal article

(Version)
Accepted Manuscript

(URL)
https://hdl.handle.net/20.500.14094/90000181

Chemical states of dodecanethiolate-passivated Au nanoparticles: Synchrotron-radiation photoelectron spectroscopy

Akinori Tanaka [a,*], Yuitsu Takeda [a], Tazumi Nagasawa [a], and Kazutoshi Takahashi [b]

[a] *Department of Physics, Graduate School of Science, Tohoku University, Aoba-ku, Sendai 980-8578, Japan*

[b] *UVSOR Facility, Institute of Molecular Science, Okazaki, Aichi 444-8585, Japan*

(Received)

We have carried out a photoemission study using synchrotron radiation of dodecanethiolate- (DT-) passivated Au nanoparticles supported on the highly oriented pyrolytic graphite (HOPG) substrates. From detailed line-shape analyses of Au 4*f* core-level photoemission spectra of DT-passivated Au nanoparticles, it is found that Au 4*f* core-level spectra consist of the two components. We attribute these components to the inner Au atoms and surface Au atoms bonded to surface dodecanethiolates. From these results, we discuss the chemical states of the present DT-passivated Au nanoparticles.

PACS codes: 71.24.+q, 73.61.Tm, 73.90.+f

Keywords: A. nanostructures, B. chemical synthesis, E. photoelectron spectroscopies, E. synchrotron radiation

* Author to whom correspondence should be addressed.
E-mail: a-tanaka@srpe.phys.tohoku.ac.jp, Fax: +81-22-217-6419

1. Introduction

Metallic nanoparticles are attracting much interest because of their distinctive physical and chemical properties found in neither bulk nor molecular/atomic systems, such as high catalytic activity [1] and Coulomb blockades [2]. Recently, the surface-passivated metallic nanoparticles have been chemically synthesized in the solution including surfactants [3, 4]. These surface-passivated nanoparticles are monodisperse and very stable at room temperature, therefore, these are suitable to characterize their fundamental size-dependent properties. Furthermore, these surface-passivated nanoparticles exhibit closed-packed nanoparticle self-assemblies on single-crystalline substrates [5, 6], and therefore it is considered that they could be important constituents of future nanostructured devices, such as single electron devices, catalysts, and ultrahigh-density memory. In order to elucidate their intriguing properties and to develop future devices, it is indispensable to characterize the chemical states of these surface-passivated metallic nanoparticles.

On the other hand, the physical and chemical properties of self-assembled monolayers (SAMs), which are self-assembled monomolecules such as the alkanethiolates on metallic single-crystal substrates, have been investigated by means of various experiments [7]. The stabilities of these SAMs have been considered to originate from the strong chemical bond at the interface between the surfactant molecules and metallic substrates. Up to now, considerable theoretical and experimental investigations were made to characterize the surfactant-substrate bonds. Among the experimental methods which clarify these issues, x-ray photoelectron spectroscopy (XPS) has been used to investigate the chemical bonds between the self-assembled alkanethiolates and metallic substrates. However, in the previous works using XPS [3, 8], almost arguments have been concentrated on sulfur core-levels of surface alkanethiolates, and furthermore no difference between the bulk atoms and interface atoms bonded to surface adsorbates of alkanethiolates has been reported in the core-level spectra of substrate metals. We believe that three reasons can explain why only a single component is observed in core-level XPS of the substrate metals. First, the number of bulk atoms which are not bonded to the surfactants largely outnumbers the surface atoms bonded to surfactants. This means

that the observed XPS spectra are dominated by the unreacted atoms in the bulk. The second and third reasons are related to the small photoionization cross-section at the relevant excitation photon energy with x-ray region [9] and a poor energy-resolution in the XPS measurements.

In this work, we have carried out a photoemission study using synchrotron-radiation of dodecanethiolate- (DT)- passivated Au nanoparticles supported on highly oriented pyrolytic graphite (HOPG) substrates. From these results, we especially discuss the chemical states of DT-passivated Au nanoparticles. Photoemission spectroscopy, especially XPS, has been used to study the electronic structures and chemical states of free nanoparticles (clusters) [10] and nanoparticles evaporated on the substrates [11-14], but to our knowledge there is no report of a synchrotron-based core-level photoemission study with high energy-resolution to date that highlights *surface-passivated* metallic nanoparticles synthesized by the chemical method. On the other hand, the nanoparticle systems have the large ratio of the number of surface and inner atoms and high surface area, indicating that the surface atoms bonded to alkanethiolate (surface-passivants) molecules largely contribute to the core-level photoemission spectra. Therefore, it is considered that this approach also contributes to the characterization of chemical bonds of SAMs on the bulk metallic substrates.

2. Experiment

The DT-passivated Au nanoparticles were synthesized by a two-phase (water-toluene) reduction method [3]. An aqueous gold-ion solution ($HAuCl_4 \bullet 3H_2O$) was mixed with a toluene solution of phase transfer catalyst, tertraoctylammonium bromide ($(C_8H_{17})_4NBr$), and consequently the gold salts were transferred into the toluene phase. This toluene phase was subsequently corrected, and a dodecanethiol ($C_{12}H_{25}SH$) and an aqueous sodium borohydride ($NaBH_4$) were added as a surface-passivant and reducing catalyst, respectively. After stirring, the toluene/nanoparticle-rich phase was corrected and was evaporated in a rotary evaporator, and then was washed three times with ethanol to remove the phase transfer catalyst, excess dodecanethiol, and reaction byproducts. This crude product

was redispersed in toluene and was annealed at 353 K with dodecanethiol, and then was washed three times again with ethanol to remove the excess dodecanethiol. After that, the product was redispersed in toluene, and finally size-selective precipitation using the toluene/ethanol as the solvent/nonsolvent pair was performed by a centrifugation to improve the nanoparticle size distribution. In this method, the nanoparticle size can be controlled by the ratio of initial Au ($HAuCl_4 \bullet 3H_2O$) and dodecanethiol. The size distributions in diameter and shapes of the synthesized DT-passivated Au nanoparticles were characterized by *ex-situ* observations with JEM-2000EXII (JEOL Co.) transmission electron microscope (TEM). The samples for TEM observations were prepared by drying the toluene dispersions of DT-passivated Au nanoparticles on the amorphous carbon coated copper TEM grids.

Photoemission measurements were carried out at BL-5A of UVSOR Facility, Institute for Molecular Science, Okazaki, Japan. For the photoemission measurements, the synthesized DT-passivated Au nanoparticles were supported on HOPG substrates by evaporating the solvent (toluene) from the dispersion of DT-passivated Au nanoparticles on the single-crystalline HOPG cleaved surface in a nitrogen-filled glove bag directly connected to the ultrahigh-vacuum photoelectron spectrometer. Then the samples were transferred into the photoemission analysis chamber without exposure to air. The cleanliness was checked by *in situ* Auger electron spectroscopy (AES). The thus-prepared samples show no AES signals from the contaminants. Photoemission measurements were performed using EA-125HR (OMICRON Co.) photoelectron spectrometer with the incident photon energy of 180 eV. The base pressure of photoelectron spectrometer was in the 10^{-9} Pa range. The photoemission spectra were recorded at room temperature, and no degradation of the samples was observed.

3. Results and Discussion

Figure 1 shows the TEM micrographs and the corresponding size distributions in diameter obtained by TEM observations for the DT-passivated Au nanoparticles used in this work. The obtained mean diameters d_m are 2.6, 3.0, 4.9, and 5.2 nm. An important point to note is that each nanoparticle is well separated from its

neighboring nanoparticles, indicating that the present Au nanoparticles are well surface-passivated by the dodecanethiol molecules.

Figure 2 shows the Au 4*f* core-level photoemission spectra of the DT-passivated Au nanoparticles with the various diameters on the HOPG substrates at room temperature measured with photon energy of $h\nu$=180 eV, compared with that of bulk Au polycrystalline evaporated film. The Au 4*f* core-level photoemission spectrum of bulk Au crystallite in Fig. 2 is almost identical with the previously reported ones [15, 16]. On the other hand, as shown in Fig. 2, the present DT-passivated Au nanoparticles exhibit the significant higher-binding-energy shifts of Au 4*f* core-level photoemission spectra, compared with the bulk Au crystallite. Furthermore, the binding energies of Au 4*f* core-level spectra seem to shift to a higher-binding-energy side with decreasing the nanoparticle diameter. In addition, Au 4*f* core-level spectra of the present DT-passivated Au nanoparticles exhibit a slightly asymmetric peak with a tail at the higher-binding-energy side, and this asymmetry increases with decreasing the nanoparticle diameter. In order to discuss the detailed spectral features, we carried out the line-shape analyses of Au $4f_{7/2}$ core-level photoemission spectra by a least-square method. Figure 3 shows the results of line-shape analyses of Au $4f_{7/2}$ core-level spectra for bulk Au crystallite and DT-passivated Au nanoparticles with various mean diameters. As previously well established [15, 16], we decomposed the Au 4*f* core-level spectrum of bulk Au crystallite into two components, which originate from the Au atoms in the bulk and topmost surface Au layer. Each peak was described by a convolution of Doniach-Sunjic line shape with a Gaussian due to the instrumental and phonon broadening. This Doniach-Sunjic line shape is characterized by a Lorentzian due to the lifetime broadening and the singularity index. The difference between the observed spectra and sum of decomposed components are also shown at the bottom in Fig. 3. As shown in Fig. 3(a), it is found that the 4*f* core-level spectrum of bulk Au crystallite is fitted fairly well by the two components corresponding to bulk and surface components, and that the observed surface core-level shift of –0.3 eV is consistent with the literature values [15, 16]. The higher-binding-energy (dotted line) and lower-binding-energy (short dashed line) peaks are bulk and surface components, respectively. On the other hand, it is found that the Au 4*f* core-level photoemission spectra of the present

DT-passivated Au nanoparticles are also reproduced by two components. Firstly, we attempted the one-component fits to Au 4*f* core-level spectra of the present DT-passivated Au nanoparticles. However, the residual is quite large in each sample compared with the case of two-components fits, and the obtained parameters of linewidths by the one-component fits are significantly different with those of bulk Au crystallites. Therefore, it is concluded that the two-components fits to Au 4*f* core-level spectra of the present DT-passivated Au nanoparticles also provide satisfactory results as shown in Fig. 3. The parameters obtained from the line-shape analyses are listed in Table I for the fairly good fits shown in Fig. 3.

From the line-shape analyses of Au $4f_{7/2}$ core-level photoemission spectra of DT-passivated Au nanoparticles, we find that the relative intensity of two-components depends on the nanoparticle diameter. That is, the relative intensity of higher-binding-energy component (long dashed line in Figs. 3(b)-(e)) to lower-binding-energy component (dotted line in Figs. 3(b)-(e)) increases with decreasing the nanoparticle diameter. The nanoparticle systems have a higher number ratio of surface atoms to atoms in bulk with decreasing the nanoparticle diameter. Furthermore, the binding energy and spectral feature of the lower-binding-energy component in each sample are similar to those of bulk component in the Au 4*f* core-level spectrum observed for bulk Au crystallite. Therefore, it is considered that the lower-binding-energy and higher-binding-energy components originate from the inner Au atoms of Au nanoparticles and the surface Au atoms of Au nanoparticles bonded to surface-passivants of DT molecules, respectively. An important point to note is that these surface components accompany with chemical shifts to higher binding energies relative to the bulk components. This indicates the different chemical states in the surface Au atoms bonded to DT molecules with the inner Au atoms and existence of a chemical reaction (chemisorption) between the surface-passivants of DT molecules and Au nanoparticles. That is, the charge transfer occurs from the core Au nanoparticles to surface-passivants of DT molecules. The reason why we can separate first time the two components in the core-level spectra due to the inner and surface atoms bonded to surface-passivants is considered to originate from the higher number ratio of surface to inner atoms in the nanoparticles and high-resolution measurements based

on the synchrotron-radiation. As shown in Table I, the chemical shifts of DT-passivated Au nanoparticles with the mean diameters of 5.2, 4.9, 3.0, 2.6 nm are 0.27, 0.27, 0.28, and 0.33 eV, respectively. The chemical shifts of surface Au atoms bonded to DT molecules increase with decreasing the nanoparticle diameter. This indicates that the bonding nature between the surface-passivants of DT molecules and Au nanoparticle surface, such as a coordination number and configuration of surface-passivants, changes with the nanoparticle diameter. The above dependence of bonding nature on the nanoparticle diameter might originate from the structural factor such as size-dependent curvature of nanoparticle surface, effect due to the existence of habit in the smaller nanoparticles, *etc*. Since the chemical shifts of surface components depend on the nanoparticle size, the broader linewidths of the surface components than those of the bulk components is considered to originate from the inhomogeneous width due to the size distributions.

In addition, the bulk components in the Au 4*f* core-level photoemission spectra of the present DT-passivated Au nanoparticle shifts to higher binding energy relative to the bulk Au crystallite. Furthermore, this energy-shift increases with decreasing the nanoparticle diameter. The final-state effect in the photoemission spectrum due to the positively charged photohole created by the photoionization has been reported in previous photoemission studies for nanoparticles [10-14, 17, 18]. When the exciting light emits a photoelectron, the photohole left behind in the nanoparticles during the time scale relevant to the photoemission process will lower the kinetic energy of photoelectrons through the Coulomb interaction. Thus, although the relaxation response within the nanoparticle may otherwise proceed normally, an excess positive charge left behind in the nanoparticle significantly induces the final-state effect in the photoemission. This final-state effect would play a more important role in the present surface-passivated Au nanoparticles supported on the substrates, since the surface-passivated nanoparticles weakly couple with the substrates through the surface-passivants. Therefore, the higher-binding-energy shifts of the bulk components in the DT-passivated Au nanoparticles are considered to originate from this final-state effect. From the static viewpoint, the kinetic energy shift of photoelectrons due to the photohole left behind in the nanoparticle is give by $\Delta E=e^2/2C$, where $C=4\pi\varepsilon_0 R_N$ is the self-capacitance of the nanoparticle with a radius

of R_N. An exact calculation shows that this energy-shift is given by $\Delta E=\alpha e^2/4\pi\varepsilon_0 R_N$ with α=0.41 for Au nanoparticle [17]. The higher-energy shifts with decreasing the nanoparticle diameter also can be qualitatively explained by this final-state effect. However, from the previous works [12, 13, 17, 18], the experimental photoemission spectra have been well characterized by a dynamic final-state effect model that takes into account the Coulomb interaction between the photoelectron and photohole with a finite tunneling time during the photoemission process. This discussion is described in detail elsewhere [12, 13, 17, 18].

4. Summary

We have performed a photoemission study using synchrotron radiation of DT-passivated Au nanoparticles supported on the HOPG substrates. From the detailed line-shape analyses of Au 4*f* core-level photoemission spectra, it is found that the Au 4*f* core-level spectra of the present DT-passivated Au nanoparticles consist of two components, which originate from the inner Au atoms of Au nanoparticles and surface Au atoms bonded to surface-passivants of DT molecules. Furthermore, it is found that the chemical-shifts of these surface components depend on the nanoparticle diameter. This indicates that the chemical states of the surface Au atoms bonded to surface-passivants of DT molecules depends on the nanoparticle diameter.

Acknowledgement

This work was supported by grants from the Ministry of Education, Culture, Sports, Science and Technology of Japan, and Advanced Technology Institute Foundation, Japan. We thank the staffs of the UVSOR Facility, Institute for Molecular Science, for their technical support.

REFERENCES

[1] M. P. A. Viegers and J. M. Trooster, Phys. Rev. B **15** (1977) 72.

[2] G. Medeiros-Ribeiro, D. A. A. Ohlberg, R. S. Williams, and J. R. Heath, Phys. Rev. B **59** (1999) 1633.

[3] M. Brust, M. Walker, D. Bethell, D. J. Schiffrin, and R. Whyman, J. Chem. Soc., Chem. Commun. **1994** (1994) 801.

[4] M. M. Alvarez, J. T. Khoury, T. G. Schaaff, M. Shafigullin, I. Vezmar, and R. L. Whetten, Chem. Phys. Lett. **266** (1997) 91.

[5] A. Taleb, V. Russier, A. Courty, and M. P. Pileni, Phys. Rev. B **59** (1999) 13350.

[6] W. D. Luedtke and U. Landman, J. Phys. Chem. **100** (1996) 13323.

[7] D. J. Wold and C. D. Frosbie, J. Am. Chem. Soc. **122** (2000) 2970.

[8] Ch. Zubragel, C. Deuper, F. Schneider, M. Neumann. M. Grunze, A. Schertel, Ch. Woll, Chem. Phys. Lett. **238** (1995) 308.

[9] J. J. Yeh and I. Lindau, Atomic Data and Nuclear Data Tables, **32** (1985) 1.

[10] M. Seidl, K.-H. Meiwes-Broer, and M. Brack, J. Chem. Phys. **95** (1991) 1295.

[11] S. L. Qiu, X. Pan, M. Strongin, and P. H. Citrin, Phys. Rev. B **36** (1987) 1292.

[12] H. Hövel, B. Grimm, M. Pollmann, and B. Reihl, Phys. Rev. Lett. **81** (1998) 4608.

[13] H. Hövel, B. Grimm, M. Pollmann, and B. Reihl, Eur. Phys. J. D **9** (1999) 595.

[14] M. G. Mason, Phys. Rev. B **27** (1983) 748.

[15] T. C. Hsieh, A. P. Shapiro, and T.-C. Chiang, Phys. Rev. B **31** (1985) 2541.

[16] P. H. Citrin, G. K. Wertheim, and Y. Baer, Phys. Rev. B **27** (1983) 3160.

[17] T. Nagasawa, A. Tanaka, H. Sasaki, Y. Kuriyama, S. Suzuki, S. Sato, and T. Sekine, Mat. Res. Soc. Symp. Proc. **704** (2002) 319-324.

[18] A. Tanaka, Y. Takeda, T. Nagasawa and S. Sato, Phys. Rev. B **67** (2003) 033101.

FIGIURE CAPTIONS

Fig. 1. TEM micrographs and size distributions in the diameter of dodecanethiolate-passivated Au nanoparticles with mean diameters d_m of 2.6 nm, 3.0 nm, 4.9 nm, and 5.2 nm.

Fig. 2. Au 4*f* core-level photoemission spectra of dodecanethiolate-passivated Au nanoparticles supported on the HOPG substrates measured with photon energy of $h\nu$=180 eV at room temperature. The mean diameter d_m is indicated on each spectrum. The top spectrum shows the Au 4*f* core-level spectra observed for bulk Au polycrystalline evaporated film for a comparison.

Fig. 3. Results of line-shape analyses for Au $4f_{7/2}$ core-level photoemission spectra of (a) bulk Au crystallite, and dodecanethiolate-passivated Au nanoparticles with mean diameter of (b) d_m=5.2 nm, (c) d_m=4.9 nm, (d) d_m=3.0 nm, and (e) d_m=2.6 nm. The observed spectrum of bulk Au crystallite is decomposed into bulk (dotted line) and surface (short dashed line) components, and those of dodecanethiolate-passivated Au nanoparticles are decomposed into bulk components (dotted lines) and surface components bonded to surface dodecanethiolates (long dashed lines). The bottom of each panel is the difference between the observed spectrum and the sum of the decomposed components.

Table I. Fitted parameters for the line-shape analyses of the Au $4f_{7/2}$ core-level photoemission spectra of bulk Au polycrystallite, and dodecanethiolate-passivated Au nanoparticles with mean diameter of d_m=5.2 nm, d_m=4.9 nm, d_m=3.0 nm, and d_m=2.6 nm. I_S is the intensity of surface component, and I_B is the intensity of bulk component.

	Binding energy (eV)	Lorenzian width (eV)	Gaussian width (eV)
Bulk Au crystallite			
Bulk component	84.00	0.30	0.45
Surface component	83.70	0.30	0.45
Dodecanethiolate-passivated Au nanoparticle			
d_m=5.2 nm			
Bulk component	84.00	0.36	0.51
Surface component	84.27	0.36	0.53
d_m=4.9 nm			
Bulk component	84.04	0.33	0.48
Surface component	84.31	0.33	0.53
d_m=3.0 nm			
Bulk component	84.27	0.32	0.47
Surface component	84.55	0.32	0.56
d_m=2.6 nm			
Bulk component	84.32	0.35	0.58
Surface component	84.65	0.35	0.60

	I_S / I_B
Dodecanethiolate-passivated Au nanoparticle	
d_m=5.2 nm	0.73
d_m=4.9 nm	0.83
d_m=3.0 nm	1.21
d_m=2.6 nm	1.31

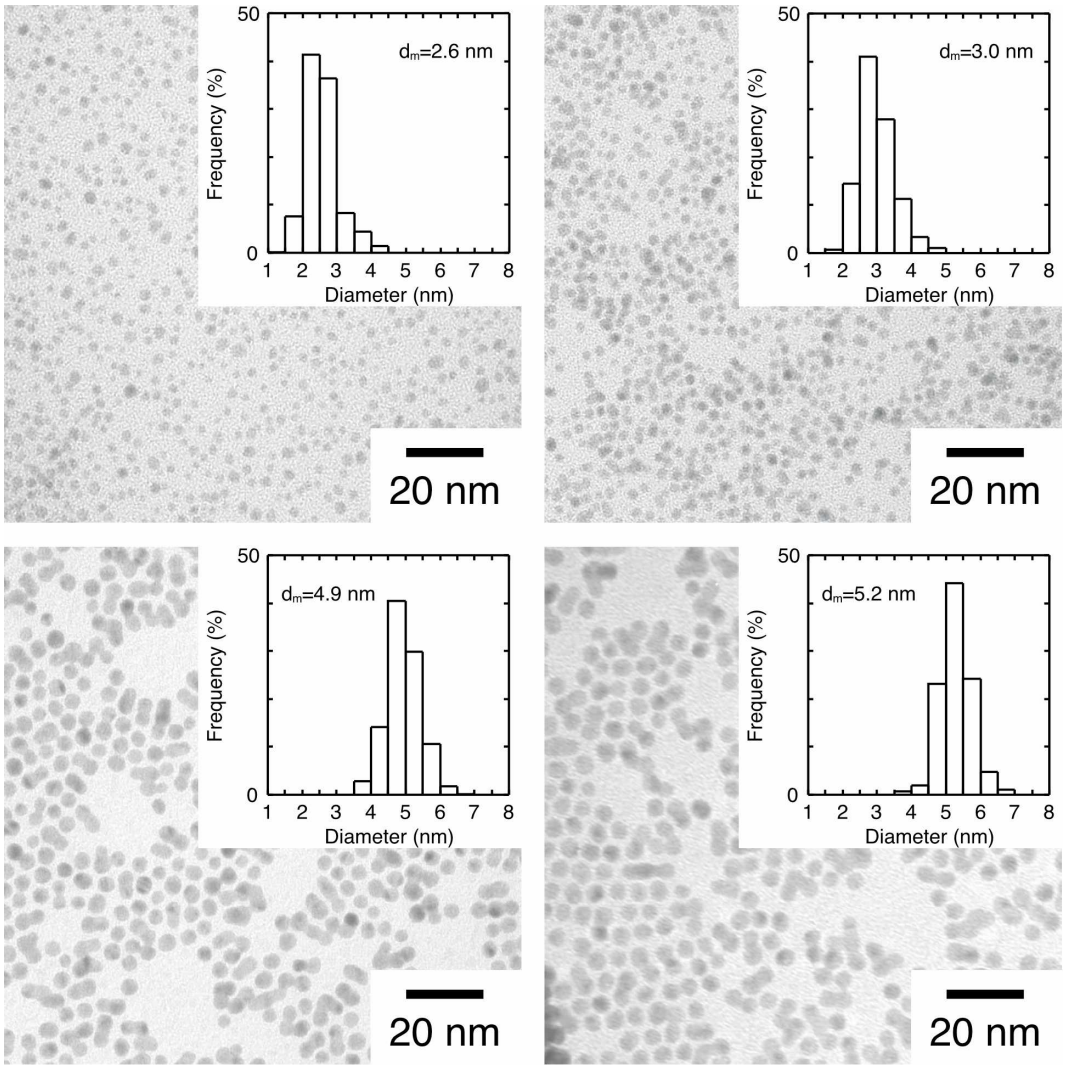

Fig. 1
A. Tanaka *et al*.

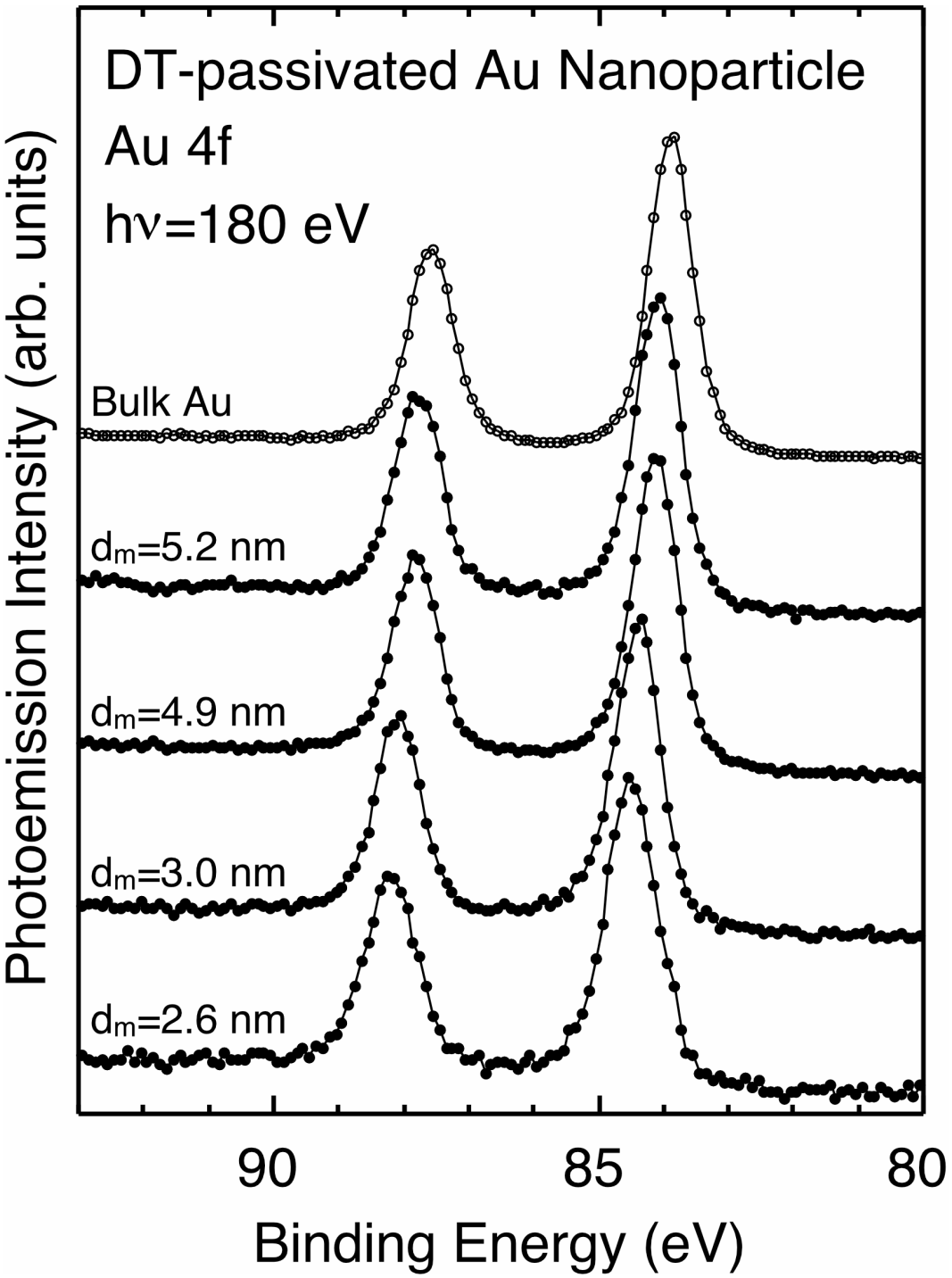

Fig. 2

A. Tanaka *et al*.

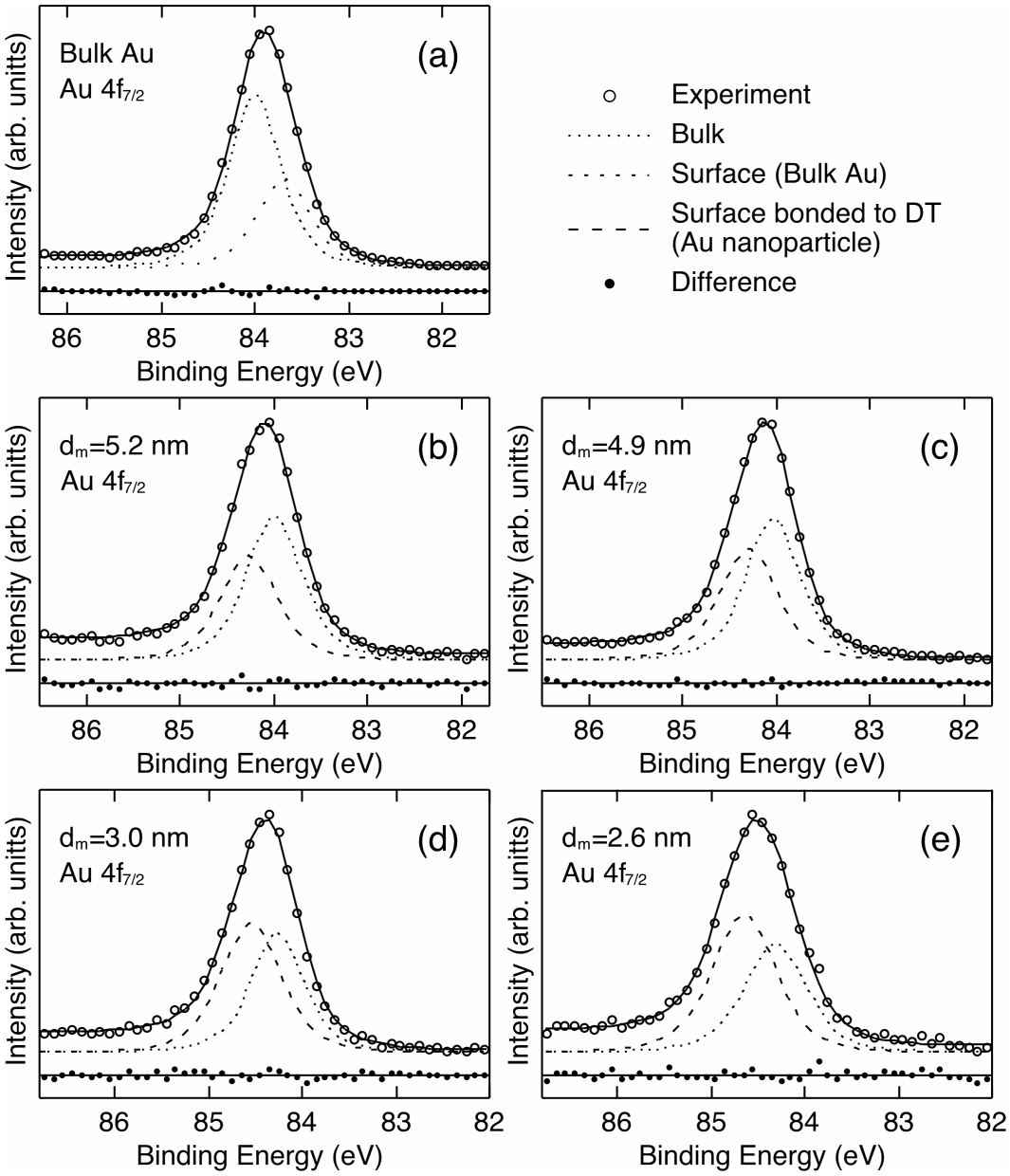

Fig. 3
A. Tanaka *et al*.